Soft Brain-Machine Interfaces for Assistive Robotics: A Novel Control Approach

Lucia Schiatti*, Jacopo Tessadori*, Giacinto Barresi, Leonardo S. Mattos, and Arash Ajoudani

***Abstract*— Robotic systems offer the possibility of improving the life quality of people with severe motor disabilities, enhancing the individual's degree of independence and interaction with the external environment. In this direction, the operator's residual functions must be exploited for the control of the robot movements and the underlying dynamic interaction through intuitive and effective human-robot interfaces. Towards this end, this work aims at exploring the potential of a novel Soft Brain-Machine Interface (BMI), suitable for dynamic execution of remote manipulation tasks for a wide range of patients. The interface is composed of an eye-tracking system, for an intuitive and reliable control of a robotic arm system's trajectories, and a Brain-Computer Interface (BCI) unit, for the control of the robot Cartesian stiffness, which determines the interaction forces between the robot and environment. The latter control is achieved by estimating in real-time a unidimensional index from user's electroencephalographic (EEG) signals, which provides the probability of a neutral or active state. This estimated state is then translated into a stiffness value for the robotic arm, allowing a reliable modulation of the robot's impedance. A preliminary evaluation of this hybrid interface concept provided evidence on the effective execution of tasks with dynamic uncertainties, demonstrating the great potential of this control method in BMI applications for self-service and clinical care.**

I. INTRODUCTION

The applications of robotic arms in assistive domains have demonstrated a high potential in improving the patient's quality of life by reducing their degree of dependence on caregivers, aiding them in activities of daily living (ADLs), such as self-care and pick-and-place tasks [1]. Patients who can benefit from this technology include those with upper body disabilities, such as traumatic spinal cord injuries (SCI), paraplegic and tetraplegic patients [2]. To make robotic arms suitable for the execution of a large class of daily tasks, intuitive and user-friendly human-robot interfaces must be designed to associate the residual capabilities of the users with disabilities to appropriate robot functions.

There are many studies aiming at improving the usability of commercially available robotic arms in assistive scenarios, by designing control interfaces able to reduce user's cognitive burden and time required to accomplish a task. Such interfaces often rely on teleoperation or shared control paradigms. Typically the partially or fully autonomous robot behavior is adapted to the user's high level inputs, based on his/her residual limb motor capabilities, to enhance the task execution performance. An example of implementation is shown in [3], where shoulder movements are detected and mapped into high level control signals for a robotic arm. Here a shared-control framework for assistive manipulation is built on the concept of autonomous piecewise trajectory segments. In a similar vein in [4], a haptic 3D joystick was adapted to directly control a robotic arm movements, enhancing the performance of traditional arm joystick control. In [5], a hand gesture recognition interface was combined with robot embedded object tracking and face recognition to control a wheelchair-mounted robotic manipulator.

However, for people suffering from more severe forms of motor disabilities, the above mentioned Body-Machine Interface examples cannot be exploited to drive a robot function. To address this issue, former studies explored the use of gaze [6] or brain signals, through eye-trackers and Brain-Computers Interfaces (BCI) respectively, to produce robot control by means of non-muscular channels. Robotic systems driven by brain signals, also known as Brain-Machine Interfaces (BMI), typically exploit P300 [7], steady-state visual evoked potentials (SSVEP) [8], or motor imagery [9] paradigms, to generate high level commands to control a robot. However, despite the continuous improvements, BCI systems are still far behind those based on Body-Machine Interfaces in terms of performance and reliability. This is due to well-known issues, such as high cognitive loads on the user, especially in continuous control schemes, low performance in high degrees of freedom control, and lack of flexibility given that user choices are mostly predefined. To overcome the limitations of pure BCI systems, hybrid interfaces have been proposed that exploit a combined use of EEG and another biosignal, as those based on BCI and gaze, to enhance communication [10] or robot control [11].

It is worth mentioning that most of the existing solutions focus on aspects related to the ease-of-use and intuitiveness of the user interface rather than on the control of physical interaction capabilities of the robot. The latter feature can contribute to enhanced interactions in the human-robot-environment loop, and the underlying safety. When developing a robotic assistive tool, a safe behavior must be guaranteed e.g., for eating/drinking or personal hygiene tasks, as well as in case of accidental arm collisions with the environment [12]. A well-known strategy to ensure safety in a robotic system is the active impedance control, which regulates the interaction between the robot and its environment, including a virtual compliance at the joint level between the motor and the output, which causes the human operator to perceive a softer arm.

Within this context, the concept of Teleimpedance control [13] has been recently proposed for the control of teleop-

All authors are with Department of Advanced Robotics at the Istituto Italiano di Tecnologia, 16163 Genova, Italy. E-mail: {lucia.schiatti, jacopo.tessadori, arash.ajoudani}@iit.it

*These authors contributed equally to this work.

erated robots, not only by means of kinematics quantities, to drive robot position and trajectory, but also regulating dynamic aspects like its stiffness or full impedance parameters during the task execution. Through this framework, the robot is able to adapt its physical behavior to various interaction scenarios, by replicating the master's real-time measured trajectories and limb impedance, usually estimated by processing electromyographic (EMG) signals [14]. Nevertheless, as mentioned above, the use of EMG cannot be considered for patients with severe motor disabilities.

To address these issues, in this work we present a hybrid BMI for real-time planning of a robotic arm movements and its physical interaction behavior. Our contribution is twofold. (1) We use gaze signals for continuous robot position control, to explicitly select the target in reaching and grasping tasks. In this way, the developed interface can be used by severely motor-impaired people, since gaze control is a long-lasting motor process in most motor diseases. Moreover, the gaze constitutes an intuitive and reliable input to control the robot motor planning in the 3D space, overcoming the limits and constraints of a BCI system, which we use instead for low-dimensional control. (2) We introduce the novel idea of exploiting EEG signals as an input for active impedance control of assistive robots. To the best of our knowledge, it is the first attempt in the literature. This approach will enable motor-impaired users to achieve also a dynamic control of the robot interaction behavior (stiff/soft). Considering this feature, we call the presented system "Soft BMI". The control of robot Cartesian stiffness profile is simultaneous to the kinematic gaze-driven position control, in a seamless way, and the BCI is used to command a less crucial aspect of robot behavior, for which an estimation error does not contribute to a substantial reduction of the robot performance.

The proposed technique is implemented in an assistive robotics application: using a robotic arm to grasp and move objects in tasks with different constraints. In our setup (see Fig. 1), the user can drive a compliant robot using gaze and move it in an unstructured environment to establish a soft contact or avoid high interaction forces during collision. If there is a requirement for a higher interaction force profile, the operator can increase the robot stiffness to accomplish the task, by means of a mental command. A unidimensional index corresponding to the probability of command detection is associated to the regulation of the robot's Cartesian stiffness components in all translational and rotational directions. This allows for a higher task accuracy, as it is well-known that an enhanced movement accuracy or increased force capability in humans or robots can be achieved by stiffer profiles of the human and the robot joints [15].

II. MATERIALS AND METHODS

Fig. 2 introduces the system, which consists of three main parts: Input block, which includes two web cameras, an eye-tracker, and an EEG headset to achieve the BCI functions; Control Interface, implemented in Processing programming environment, for the real-time processing of the input data to generate suitable control outputs for the third block; and

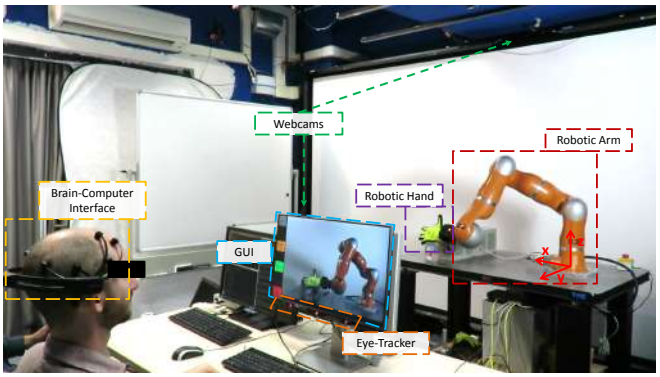

Fig. 1. System setup for Soft Brain-Machine Interface: robot translational movements in space are controlled by human gaze, while an EEG-driven unidimensional index regulates the robot Cartesian stiffness in real-time.

the Actuated System, a 7-DoF torque controlled robotic arm equipped with the Pisa/IIT SoftHand [16]. The components of the system and the flow of information between them are described in detail in the following sub-sections.

A. Web cameras

Two low cost Logitech web cams were used to monitor the robot position from different angles and allow the user to plan 3D translational movements of the robot end-effector. Cameras were placed on top and to the side of the setup, so that each view allows for a clear selection of a coordinate pair. A Logitech B525 HD webcam was set above the robot, to capture xy view in robot coordinates system (view 1 in Fig. 3), while a Logitech HD C270 webcam was put in front of the robot, to catch xz view (view 2 in Fig. 3). An autonomous algorithm was implemented to build the mapping from the gaze coordinates on the screen to the robot coordinates for each camera. To this purpose, in the calibration phase (executed only once, depending on the placement of the cameras), the operator selected a few points on the screen, with known coordinates on the KUKA frame of reference, for each view. The rest of the mapping, i.e. the identification of two homogeneous transformations, was done autonomously using the algorithm.

B. Eye-Tracker

The eye-tracker employed in this work was the commercially available Tobii EyeX, both in its hardware and software (i.e. EyeX SDK) components. The system consists of two infrared micro-projectors that are used to illuminate user's eyes, while two optical cameras record the reflections of visible and infrared light on corneas and pupils. A USB 3.0 connection is required to connect the sensor system to the computer, in order to transfer the data collected by the imaging sensor. This information is processed by the dedicated software to provide the screen coordinates of the user's current gaze target. The gaze target coordinates provided by the Tobii system were transmitted via UDP to the Control Interface script at 30 Hz frequency, and filtered using the following equation:

$$X_i(t) = X_i(t-1)(1-\sqrt{V(t)}) + U_i(t)\sqrt{V(t)} \quad (1)$$

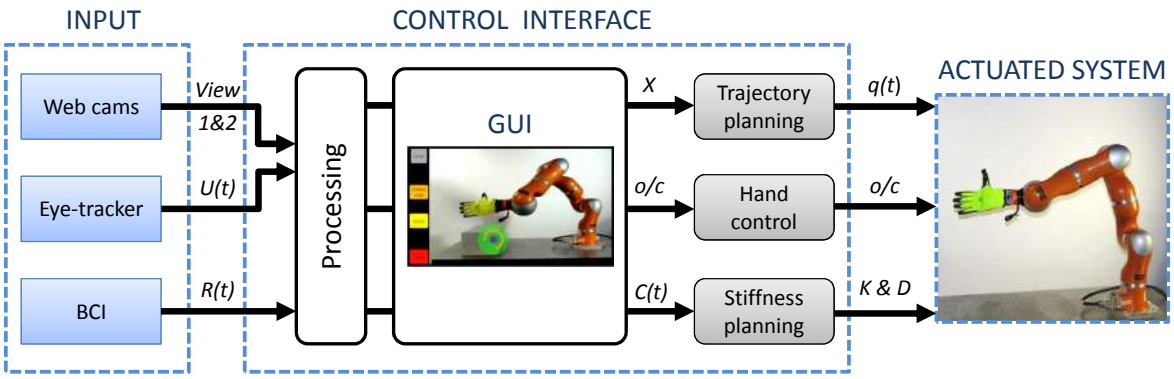

Fig. 2. Information workflow between system components.

in which X_i denotes the filtered i^{th} coordinate, with i=1,2, $U_i(t)$ is the Tobii estimation at time t and $V(t)$ is an estimation of the movement speed of the gaze target in the current step. More specifically, $V(t)$ was defined as:

$$V(t) = \sqrt{\sum_{i=1,2} \left(\frac{X_i(t-1) - U_i(t)}{X_{max_i}} \right)^2} \qquad (2)$$

where X_{max_i} is the largest value the i^{th} coordinate can assume (i.e. the screen resolution along each dimension). With this normalization, $V(t)$ varies in the $[0, 1]$ range. Intuitively, this filter was designed to cancel out minor gaze fluctuations, while leaving performance on fast movements as unchanged as possible.

C. Brain-Computer Interface

The unidimensional index for the impedance control was estimated through the combined use of the EEG system Emotiv EPOC+ and its accompanying software. The Emotiv EPOC+ is a low cost EEG wireless headset with 14 electrodes located at the positions AF3, F7, F3, FC5, T7, P7, O1, O2, P8, T8, FC6, F4, F8, AF4 according to the International 10-20 system, communicating with the PC via bluetooth. Sampling rate is 256Hz. Given the final goal of developing an affordable and usable assistive technology, Emotiv EPOC was chosen in this study for his significant advantages in terms of cost, portability, robustness and user customization. Although it lacks in reliability and signal quality compared to existing medical EEG interfaces, it has already been used in robotic applications both exploiting its embedded muscular measurements [17] and EEG signals (to control a 7 dof robotic arm [18]).

The Emotiv software includes a control panel, which encompasses a Cognitiv suite. The latter evaluates user's real time brainwave activity to discern the user's conscious intent to perform physical actions on a real or virtual object. Up to four actions can be recognized at any given time. The detection system outputs a single action or neutral (i.e. no action) at a time, along with an action power, a unidimensional scalar index ranging between 0 and 1 representing the detection certainty that the user has entered the mental state associated with that action. For the present work, only one action, corresponding to the "push" mental command was trained and used. Training was performed using the Cognitiv suite, and consisted in alternation of neutral and active states in trials lasting 8 s each one, for some minutes, until user felt comfortable with the state control. In neutral trials the user was asked to relax and avoid moving, while during active trials the user had to focus on the action of pushing a 3D object (cube) represented on the screen.

An open source software (Mind Your OSCs) was adopted to transmit via OSC protocol the Emotiv readings to the Processing Control Interface. To limit quick fluctuations in the estimation of the mental action state index, the raw value provided by the Cognitiv suite was low-pass filtered with a leaky integrator:

$$C(t) = min(1, R(t) + A \times C(t-1)) \qquad (3)$$

Here, $R(t)$ is the reading provided by the Emotiv system at time t, while $C(t)$ is the filtered index describing user's concentration (neutral or active) state. The parameter A has a value ranging in the $[0, 1]$ interval, with typical values around 0.5. This parameter was introduced in order to compensate for widely varying performances observed across different users and sessions and it was re-calibrated before each session in order to provide an acceptable user experience. Finally, the upper limit of 1 was imposed to the C value in order to keep its range consistent with the input variable R.

D. Graphical User Interface (GUI)

The GUI itself consisted of a vertical panel on the left margin of the screen including four buttons (from top to bottom: calibration start/stop, change view, open/close and stop), while most of the monitor was displaying the live feed from the currently selected camera (Fig. 3). The buttons on the left allowed the user to:

- start and stop the calibration to map each web-cam screen view coordinates with corresponding robot workspace coordinates;
- switch currently selected camera;
- open or close the Pisa/IIT SoftHand;
- stop the robot movement in case of wrongly issued command.

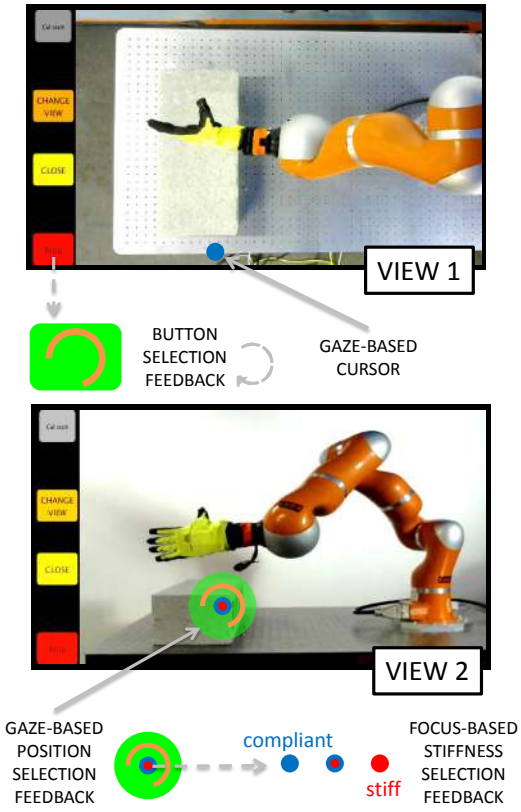

Fig. 3. Graphical User Interface.

An interactive cursor was constantly indicating gaze target and current mental state: the cursor was a blue dot when C was zero (neutral state) and it progressively became red with increasing current values of C. A button was selected when the gaze-controlled cursor rested within it for longer than 1.5 s (this dwell time was shortened to 0.5 s for the stop button in the lower left corner). A circular progress bar provided the indication of elapsed and total dwell time required.

The selection of the desired target robot position was enabled by fixing gaze on the corresponding point in the webcam screen view: if gaze velocity $V(t)$ fell below a certain threshold while on top of a specific point on the webcam image, a virtual circular button appeared and its progress bar started filling as for the buttons of the left panel. If the user did not divert its gaze from the button, when the bar was filled the target point coordinates X were sent to the robot controller. Diverting gaze caused the virtual button to disappear. Rigidity of the robot during each movement was a function (see text below) of the concentration index C at the time instant in which the progress bar filled completely.

E. Actuated System

System evaluation was carried out using a 7-DoF KUKA lightweight robotic arm. The robot was controlled in torque mode and a Cartesian impedance controller was developed to achieve the operator's planned trajectories through the eye-tracker, in KUKA frame of reference (using two transformations, as explained above). A fifth order polynomial model generated online smooth Cartesian trajectories in between two selected points on the screen, every time the operator's gaze target point on screen was detected by the User Interface. This consideration was to achieve smooth trajectories in a suitable time, that was estimated according to the distance from the final destination.

The Cartesian stiffness of the robot was allowed to vary between a minimum (K_0) and maximum (K_m) value of 300 to 2000 $\frac{N}{m}$ for all translational components (k_t), and 50 to 250 $\frac{Nm}{\text{rad}}$ for rotational ones (k_r), respectively. The exact value was estimated in real-time from the concentration index, using a linear mapping:

$$K_{t,r} = K_{0_{t,r}} + C(t)(K_{m_{t,r}} - K_{0_{t,r}}) \tag{4}$$

This profile enables the robot to establish a soft contact in case of lower stiffness values, while demonstrating a stiff behaviour when a higher precision or force generation is required by the task. The Cartesian damping matrix D was obtained from the desired K using the double diagonalisation design as explained in [19].

The robot was equipped with the Pisa/IIT SoftHand, an under-actuated and synergy driven robotic hand. The embedded adaptivity of the robotic hand made this choice ideal for the grasping of objects with various shapes since only one actuator input was controlled. The hand unit and power driver for the motors (SoftHand and force feedback cuff) are custom control boards based on the Texas Instruments Luminary DSP chip LM3S8962. The DSP control loop is executed at 1KHz while the communication with the host PC is achieved through a real time Ethernet link. Motor current measurement is performed by a hall effect based current sensor (ACS714, Allegro Microsystems Inc.) and appropriate signal conditioning integrated in the motor power driver module. The robot control script was implemented in C++ environment, running in a separate PC and receiving the user input from the Processing script via UDP. A data package included the selected target gaze coordinates X with a flag indicating if they are expressed in view 1 or view 2, a control bit indicating open or close state of the hand, and the concentration index $C(t)$ describing user's mental state.

III. SYSTEM EVALUATION

The presented Soft BMI system was tested on two different subjects (aged 24 and 33), who were asked to control the robot in two different tasks. One subject had previous experience with both the Tobii eye tracker and the Emotiv BCI system, while the second was a naive subject. Operative tests were preceded by a calibration session for both the eye-tracker and the BCI, with the standard procedures implemented in the software suites of the two systems. Both subjects were able to control the GUI of the robot within minutes: they could deliberately fixate gaze on any given point on the screen in order to select it as a robot target position while maintaining the chosen mental state, corresponding to concentration index equal to 0 for neutral or a scalar between 0 and 1 for active state, or divert gaze to prevent undesired commands.

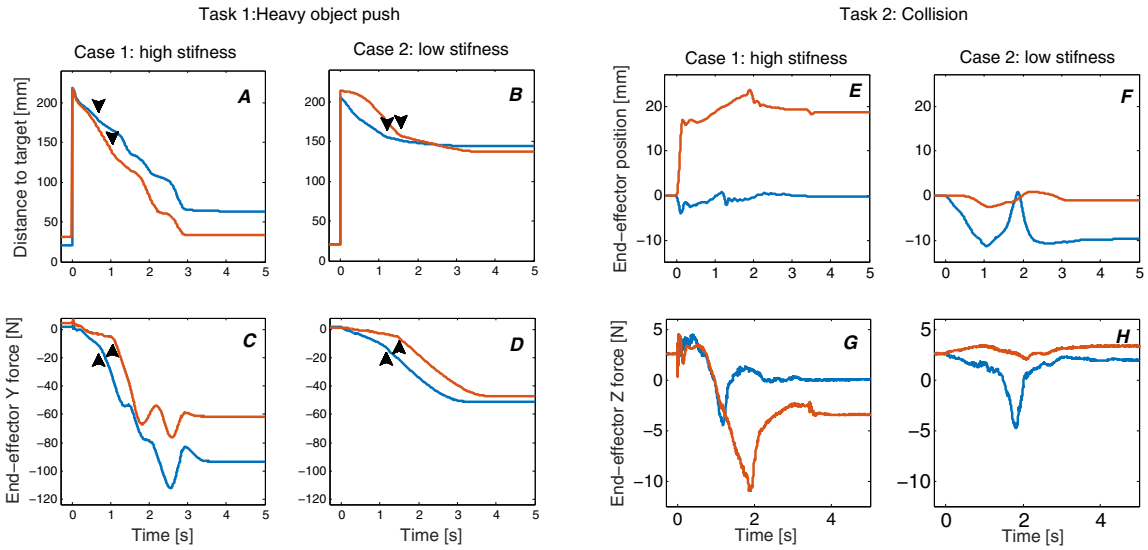

(a) (b)

Fig. 4. Results from system evaluation. Panels A-B: distance between current arm endpoint and selected target for high (panel A) and low (panel B) stiffness trials and corresponding estimated endpoint forces in the push direction (panels C-D). t = 0 corresponds to Kuka receiving movement command. Black triangles indicate the approximate contact moment between soft hand and object. Panels E-H: distance traveled by arm endpoint since t = 0 in the vertical direction, for high (panel E) and low (panel F) stiffness trials and corresponding estimated endpoint forces, in the vertical direction. t = 0 corresponds to Kuka receiving movement command. Contact between grasped object and obstacle occurs almost immediately after movement start. Blue (orange) line depicts trials performed by experienced (naive) user (S1, S2 respectively).

A. Tasks

Two complementary tasks were considered to evaluate the effectiveness of the proposed interface for the online control of the robot trajectories and physical interaction behavior.

Heavy object pushing: The purpose of this task was to demonstrate the need for force production capabilities of robots when dealing with precision tasks. In this task, the user was asked to position the robotic hand beside a heavy brick (about 8 kg), and push it aside by selecting a target position around 15 - 20 cm inside the brick from the top view (please refer to the accompanying video, see Fig.5 caption). The user was asked to perform the task in both neutral and active mental state in order to select low and high robot Cartesian stiffness profile, until the task was accomplished.

Object grasping and environment collision: This task was designed to stress the need for a compliant behavior of the robot when dealing with an unstructured environment, in which collisions with obstacles are likely to occur. The user was requested to control the robot in order to grasp a partly full plastic water bottle (around 0.2 kg), lift it and then move the arm such that the part of the bottle sticking out below the hand would hit a rigid, immovable obstacle. As for the previous task, the user was asked to repeat this test in two conditions, with the lowest and highest possible levels of robot stiffness respectively. Our objective was to examine the effectiveness of the proposed interface in allowing the user to control robot behavior adaptability to the environment constraints.

B. Results and Discussion

Heavy object pushing: Fig. 4 illustrates results of two repetitions of the task, performed by the two subjects. Panels A-C and B-D represent data collected during the active and neutral mental state, corresponding to high and low stiffness respectively. In particular, panels A and B show the distance, expressed in millimeters, between gaze-selected target and robot endpoint current position, while the second row presents the endpoint forces produced by the Kuka robot in the y (pushing) direction. Different colors correspond to trials performed by different subjects.

Since the robot started in the position of the last selected target, the distance to target was approximately 0 at the beginning of the trial. At $t = 0$, a new target was chosen in order to push the object forward and the robot started moving. Impact occurred around 1 s later in all presented trials, as evidenced by the black triangles in Fig. 4. After touching the obstacle, the robot sharply increased the applied force in y direction to reach its intended target, as visible from the sharp change in force slope, in panels C-D (see Fig. 5 upper block for the snapshots of this experiment). In the high stiffness case ($C = 0.8, 1$ at the moment of selection for subject S1, S2 respectively), the total force produced was high enough to overcome statical friction between the object and the underlying surface, and a stick-slip movement phase occurred, characterized by oscillations in force and irregular robot speed, until the endpoint was close to its final intended target. In the low stiffness scenario ($C = 0$ for both subjects at the moment of selection) the applied force was sufficient to distend the fingers of the SoftHand (hence the small reduction in distance to target after reaching the object, panel B), but never overcame the static friction threshold. It is worth noting that even in the high stiffness case the robot was not perfectly rigid and therefore it stopped slightly short of its target and it kept applying force against the obstacle.

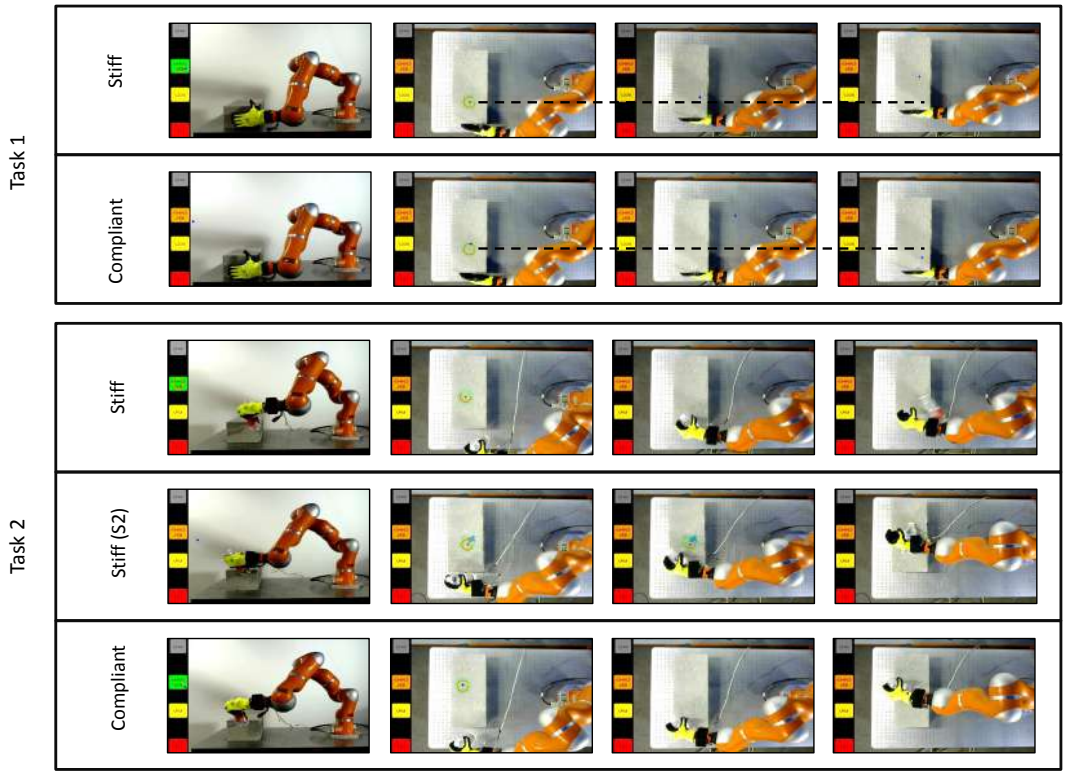

Fig. 5. Screen shots of the heavy object pushing (Task 1) and collision (Task 2) tasks in active mental state (stiff) and neutral mental state (compliant). For the second task, two different examples of the active (stiff) case for the two subjects are provided. At the link https://www.youtube.com/watch?v=k6DyosvWB_s a video of the system evaluation is available.

Object grasping and environment collision: Similarly to the previous case, subjects performed the task in two conditions: panels E-G on Fig. 4 display results for a high-stiffness (active mental state) trial, while panels F-H on the right side present the low-stiffness (neutral mental state) case. The first row shows the z coordinate of the Kuka endpoint recorded starting from the moment of the impact of the grasped object against an obstacle, while panels G and H show the corresponding estimated forces in vertical z direction.

As before, $t = 0$ indicates the time in which the movement command is received by the robot. Impact against the obstacle occurred almost immediately, with very different outcomes depending on robot arm rigidity: for both subjects low-stiffness trials ($C = 0$) resulted in the bottle being successfully held on to, whereas high-stiffness trials ($C = 1$) resulted in the dislodgement of the bottle from the soft hand grip. Moreover, the high-stiffness case present a strong difference for the two subjects: in the case of subject 1 (S1, blue line), the bottle rolled away after being dislodged, whereas for subject 2 (S2, orange line) the plastic bottle was stuck between the robot arm and the brick (see Fig. 5 lower block for the snapshots of this experiment). The different behavior is clearly shown in the graphs: in the stuck-bottle case (panel E, orange line), the robot endpoint was sharply pushed upwards by the bottle itself, while for the rolling-bottle case (panel E, blue line) the impact caused only a minor readjustment in the robot trajectory. The corresponding force graph (panel G) shows a value of about 2.5 N at the beginning of both subjects trials, which was force required to keep the bottle lifted and steady. During the impact, forces at the endpoint turned negative, as the distal end of the robot arm was pushed upwards by the interaction between held bottle and obstacle. After the bottle was dislodged, the estimated force was around 0 N if the bottle rolled away (blue line) or negative when the robot was actually pushing downwards on the stuck bottle (orange line).

In the low stiffness case, the bottle remained within the hand for the whole trial, as the robot arm adapted its path according to the imposed environment constraints. In particular the robot endpoint moved downward when it was rotating around the bottle-obstacle contact point for both users (first negative peak, panel F), then it moved slightly above target as the bottle was dragged on the surface of the obstacle (positive peak, panel F). The final position of the robot endpoint, as well as the forces expressed at the end of the trial (panel H), vary slightly according to the final relative angle between the bottle and the obstacle it was resting on.

IV. CONCLUSIONS

In this paper, a preliminary study demonstrated the possibility of controlling both kinematic and dynamic parameters of a robotic arm through a hybrid BMI - Soft BMI - that only exploits eye-movements and brain signals. These features allow the interface to be accessible to patients with sever motor disabilities, where residual muscular functions (excluding ocular control) cannot be exploited. The main contribution,

compared to the state of the art of brain-controlled assistive robotics, lies in the introduction of an additional degree of control for the user, enabling the adaptivity of the robot behavior during physical interactions with the environment.

The eye-tracking system is very intuitive in its use, as it can be calibrated and proficiently driven by a user with no previous experience within minutes, while maintaining a high degree of precision in the selection of desired targets. On the other hand, the BMI was designed in order to take advantage of the fact that tasks requiring a higher degree of mental concentration are typically those that require stiffer movements (e.g. very precise displacements or heavy object moving). Therefore the robot has a default soft and safe behavior. The BCI channel is normally inactive, and it is just used in tasks where high accuracy is required. Compared to systems where the eye-tracker alone is used for position control, this introduces a remarkable advantage. During a drawing/writing task, for instance, as the one presented in [6], a stiff behavior is advisable. On the other hand, when changing task, e.g. to self-feeding, robot stiffness should be reconfigured to a lower level by a caregiver, to allow safety. The solution proposed in this study, allows for a further degree of control and therefore independence for the patient.

The control of the robot proved to be quite easy to learn, as a naive subject learned to perform a relatively complex task such as grabbing an object and moving it around with a given degree of rigidity within his first session. At the moment, however, evoking a desired mental command required effort from the user and, sometimes, multiple attempts. This could be ascribed to the limitations connected to the use of the commercial EPOC software and hardware. Future work will be consequently devoted to re-implement the presented impedance control using the detection of EEG activity related to motor imagery, and making use of a medical EEG acquisition system. This will allow to explore the feasibility of controlling multiple degrees of freedom via BCI, as well as to enable the user to vary robot stiffness in real-time also within the same trial. A systematic study will be then carried out to experimentally evaluate the proposed interface compared to other existing approaches (solely gaze-based and BCI based), during the execution of various tasks with increasing difficulty performed both by healthy and impaired subjects.

The controller presented in this work was intended as a proof of concept for a novel kind of interface that could help to integrate a higher degree of autonomy in assistive applications of soft robotics for severely disabled patients.

V. ACKNOWLEDGEMENT

This research has been partially funded by Fondazione Roma under the grant agreement supporting TEEP-SLA project, and by the EU H2020-ICT-2015 SoftPro project.

REFERENCES

[1] K. M. Tsui, H. A. Yanco, D. J. Feil-Seifer, and M. J. Matarić, "Survey of domain-specific performance measures in assistive robotic technology," in *Proceedings of the 8th Workshop on Performance Metrics for Intelligent Systems*. ACM, 2008, pp. 116–123.

[2] D.-J. Kim, R. Hazlett-Knudsen, H. Culver-Godfrey, G. Rucks, T. Cunningham, D. Portee, J. Bricout, Z. Wang, and A. Behal, "How autonomy impacts performance and satisfaction: Results from a study with spinal cord injured subjects using an assistive robot," *IEEE Transactions on Systems, Man, and Cybernetics-Part A: Systems and Humans*, vol. 42, no. 1, pp. 2–14, 2012.

[3] S. Jain, A. Farshchiansadegh, A. Broad, F. Abdollahi, F. Mussa-Ivaldi, and B. Argall, "Assistive robotic manipulation through shared autonomy and a body-machine interface," in *Rehabilitation Robotics (ICORR), 2015 IEEE International Conference on*. IEEE, 2015, pp. 526–531.

[4] H. Jiang, J. P. Wachs, M. Pendergast, and B. S. Duerstock, "3d joystick for robotic arm control by individuals with high level spinal cord injuries," in *Rehabilitation Robotics (ICORR), 2013 IEEE International Conference on*. IEEE, 2013, pp. 1–5.

[5] H. Jiang, J. P. Wachs, and B. S. Duerstock, "Integrated vision-based robotic arm interface for operators with upper limb mobility impairments," in *Rehabilitation Robotics (ICORR), 2013 IEEE International Conference on*. IEEE, 2013, pp. 1–6.

[6] S. Dziemian, W. W. Abbott, and A. A. Faisal, "Gaze-based teleprosthetic enables intuitive continuous control of complex robot arm use: Writing & drawing," in *Biomedical Robotics and Biomechatronics (BioRob), 2016 6th IEEE International Conference on*. IEEE, 2016, pp. 1277–1282.

[7] M. Palankar, K. J. De Laurentis, R. Alqasemi, E. Veras, R. Dubey, Y. Arbel, and E. Donchin, "Control of a 9-dof wheelchair-mounted robotic arm system using a p300 brain computer interface: Initial experiments," in *Robotics and Biomimetics, 2008. ROBIO 2008. IEEE International Conference on*. IEEE, 2009, pp. 348–353.

[8] D. Petit, P. Gergondet, A. Cherubini, M. Meilland, A. I. Comport, and A. Kheddar, "Navigation assistance for a bci-controlled humanoid robot," in *Cyber Technology in Automation, Control, and Intelligent Systems (CYBER), 2014 IEEE 4th Annual International Conference on*. IEEE, 2014, pp. 246–251.

[9] J. Meng, S. Zhang, A. Bekyo, J. Olsoe, B. Baxter, and B. He, "Noninvasive electroencephalogram based control of a robotic arm for reach and grasp tasks," *Scientific Reports*, vol. 6, 2016.

[10] G. Barresi, J. Tessadori, L. Schiatti, D. Mazzanti, D. G. Caldwell, and L. S. Mattos, "Focus-sensitive dwell time in eyebci: Pilot study," in *Computer Science and Electronic Engineering (CEEC), 2016 8th*. IEEE, 2016, pp. 54–59.

[11] H. Wang, X. Dong, Z. Chen, and B. E. Shi, "Hybrid gaze/eeg brain computer interface for robot arm control on a pick and place task," in *Engineering in Medicine and Biology Society (EMBC), 2015 37th Annual International Conference of the IEEE*. IEEE, 2015, pp. 1476–1479.

[12] J. Vogel, S. Haddadin, B. Jarosiewicz, J. D. Simeral, D. Bacher, L. R. Hochberg, J. P. Donoghue, and P. van der Smagt, "An assistive decision-and-control architecture for force-sensitive hand–arm systems driven by human–machine interfaces," *The International Journal of Robotics Research*, vol. 34, no. 6, pp. 763–780, 2015.

[13] A. Ajoudani, N. G. Tsagarakis, and A. Bicchi, "Tele-impedance: Teleoperation with impedance regulation using a body-machine interface," *The International Journal of Robotics Research*, p. 0278364912464668, 2012.

[14] A. Ajoudani, *Transferring Human Impedance Regulation Skills to Robots*. Springer, 2016.

[15] P. L. Gribble, L. I. Mullin, N. Cothros, and A. Mattar, "Role of cocontraction in arm movement accuracy," *Journal of neurophysiology*, vol. 89, no. 5, pp. 2396–2405, 2003.

[16] M. G. Catalano, G. Grioli, E. Farnioli, A. Serio, C. Piazza, and A. Bicchi, "Adaptive synergies for the design and control of the pisa/iit softhand," *The International Journal of Robotics Research*, vol. 33, no. 5, pp. 768–782, 2014.

[17] G. Ranky and S. Adamovich, "Analysis of a commercial eeg device for the control of a robot arm," in *Bioengineering Conference, Proceedings of the 2010 IEEE 36th Annual Northeast*. IEEE, 2010, pp. 1–2.

[18] W. Ouyang, K. Cashion, and V. K. Asari, "Electroencephelograph based brain machine interface for controlling a robotic arm," in *Applied Imagery Pattern Recognition Workshop (AIPR): Sensing for Control and Augmentation, 2013 IEEE*. IEEE, 2013, pp. 1–7.

[19] A. Albu-Schäffer, C. Ott, U. Frese, and G. Hirzinger, "Cartesian impedance control of redundant robots: recent results with the DLR-light-weight-arms," in *IEEE Intl. Conf. on Robotics and Automation (ICRA)*, vol. 3, Sept 2003, pp. 3704–3709.